Miscibility gap and phonon thermodynamics of Fe-Au alloys studied by inelastic neutron scattering and nuclear-resonant inelastic x-ray scattering

Jorge A. Muñoz and Brent Fultz

Citation: AIP Conference Proceedings **1671**, 020001 (2015); doi: 10.1063/1.4927178
View online: http://dx.doi.org/10.1063/1.4927178
View Table of Contents: http://scitation.aip.org/content/aip/proceeding/aipcp/1671?ver=pdfcov
Published by the AIP Publishing

Miscibility gap and phonon thermodynamics of Fe-Au alloys studied by inelastic neutron scattering and nuclear-resonant inelastic x-ray scattering

Jorge A. Muñoz* and Brent Fultz†

*Intel Corporation, Information Technology Research, Hillsboro, OR 97124
†California Institute of Technology, Department of Applied Physics and Materials Science, Pasadena, CA 91125

Abstract. Recent measurements of the phonon spectra of several Au-rich alloys of face-centered-cubic Fe-Au using inelastic neutron scattering and nuclear-resonant inelastic x-ray scattering are summarized. The Wills-Harrison model, accounting for charge transfer upon alloying, is used to explain the observed negative excess vibrational entropy of mixing, which increases the miscibility gap temperature in the system by an estimated maximum of 550 K and we adjudicate to a charge transfer from the Fe to the Au atoms that results in an increase in the electron density in the free-electron-like states and in stronger *sd*-hybridization. When Au is the solvent, this softens the Fe–Fe bonds but stiffens the Au–Au and Au–Fe bonds which results in a net stiffening relative to the elemental components.

Keywords: Alloy thermodynamics, FeAu, inelastic neutron scattering, nuclear-resonant inelastic x-ray scattering
PACS: 63.20.dd, 63.20.Pw, 71.20.Be, 75.50.Bb

INTRODUCTION

In thermodynamic equilibrium, the type and proportion of the elemental components of a system determine its phase and many of its properties. The stable phase minimizes the free energy $F = U - TS$, where U is the internal energy, T is the temperature, and S is the entropy. Historically, S has been obtained indirectly from the heat capacity, but this does not allow to easily separate the contributions from the phonons, the electrons and the magnetism, making a fundamental understanding of their interactions more difficult, especially at elevated temperatures or close to phase transitions [1]. Recent developments in accelerator physics, experimental techniques, instruments, and sample environments have enabled detailed and systematic studies of phonons in a large and growing number of systems, and these studies can provide detailed information on many of their trends that can be directly compared to predictions from first principles calculations. Inelastic neutron scattering (INS) and nuclear-resonant inelastic x-ray scattering (NRIXS) are currently two of the state-of-the-art techniques to measure phonon spectra, from which the phonon or vibrational entropy S_{vib} can be obtained. For certain systems, INS and NRIXS are complementary. This is because spectra acquired using neutrons is weighted by the neutron scattering cross-section of each atom in the system, while NRIXS is a technique that probes exclusively the motions of a particular Mössbauer isotope in the system. For binary alloys containing Fe, combining results from both techniques allows an accurate, i.e., neutron-weight-corrected, determination of the total phonon density-of-states (DOS) curves as well as element-specific partial phonon DOS curves. This detailed information is helpful in assessing the relative contributions of the different components of the system to S_{vib} and in studying their individual behaviors.

In systems with segregation tendencies, contributions to S that are not configurational in origin can be comparable to the large entropy gain that comes from mixing. Properties such as the solubility limit and the miscibility gap depend on all available sources of entropy. In NiAu, a well characterized alloy with a miscibility gap temperature of about 1050 K [2], the total configurational entropy accounts for only one-half of the total entropy of mixing [3] and several computational assessments of the miscibility gap temperature that took into account only configurational contributions to the free energy overestimated it by as much as a factor of two [4, 5, 6]. The magnetic and electronic contributions to the free energy are small in NiAu [7, 8], so the excess entropy of mixing is vibrational in origin and it decreases the miscibility gap temperature by about 1000 K [3]. A recent computational study of the compositional trends in the Ni-Cu system found the vibrational entropy of mixing to be negative, favoring chemical un-mixing [9]. Other phenomena in segregating systems where S_{vib} is chief include the spinodal decomposition in FeCr [10] and the retrograde solubility in several dilute vanadium alloys [11].

Radiation Physics
AIP Conf. Proc. 1671, 020001-1–020001-9; doi: 10.1063/1.4927178

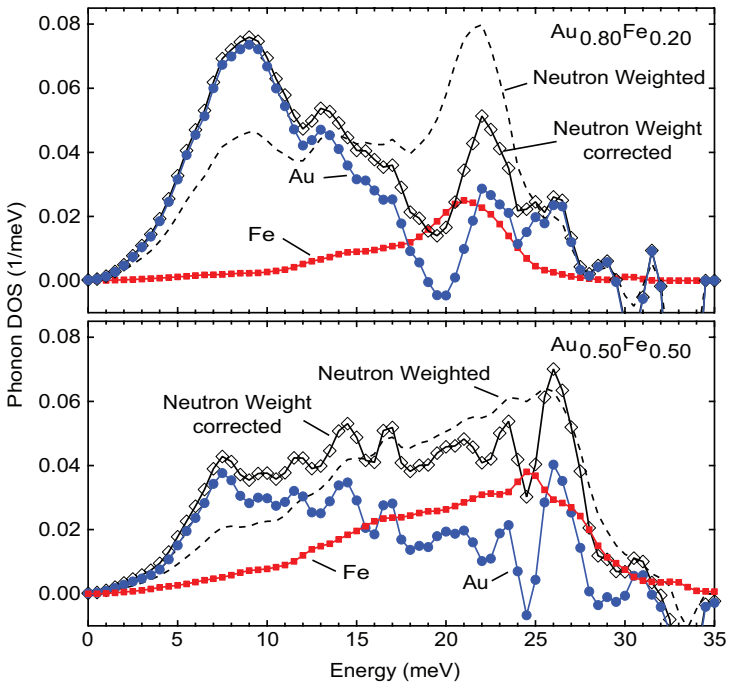

FIGURE 1. (color online) Neutron-weighted (dashed curves without markers) and neutron-weight-corrected (open diamonds) phonon DOS curves, along with the concentration weighted Fe (solid squares) and Au (solid circles) partial phonon DOS curves for $Fe_{0.20}Au_{0.80}$ (top) and $Fe_{0.50}Au_{0.50}$ (bottom).

Fe and Au are of major importance in industry and technology and the scientific literature on the Fe-Au system is vast, but bulk mixtures of Au and Fe atoms are largely immiscible at low temperatures. The lifetime of alloys quenched from high temperatures ranges from days to months depending on the composition [12]. In a recent publication [13] which included the INS and NRIXS measurements on the Fe-Au system shown here and also an analysis of the electronic structures and calculations of the phonons at several compositions based on density functional theory, we showed that there is a large increase in the average phonon energy (stiffening) of the Au partial phonon DOS with Fe concentration and that this is a highly local effect produced by an increase in the electron density of the free-electron-like states and by stronger *sd*-hybridization. Since then, a similar stiffening was predicted for the Cu vibrations in the Ni-Cu system with increasing Ni concentration and a softening [9] and this effect likely has the same origin. Here we expand the analysis of the thermodynamics of the Fe-Au system and use the Wills-Harrison model [14] to show how the charge transfer from the Fe to the Au atoms differentially affects the stiffness of the Au–Au, Au–Fe and Fe–Fe bonds and contributes to the low miscibility between Fe and Au when Au is the solvent. The Fe–Au bonds are inherently soft and should favor mixing, but in the Au-rich part of the phase diagram, charge transfers result in a stiffening of the bonds between Au atoms surrounding an Fe atom that is large enough to favor un-mixing. Based on the proportion of bonds, the bond stiffening should have a maximum at concentrations close to 20 at.% Fe, which corresponds to a minima in the excess vibrational entropy of mixing observed experimentally. The vibrational entropy increases the miscibility gap temperature by as much as a factor of 4 (about 550 K), with a maximum at 10 at.% Fe, although the effect is smaller for higher Fe contents and reaches zero at around the equiatomic composition. Phonon anharmonicity is not explicitly considered in the current analysis, but it has been observed to be significant in other systems with segregation tendencies such as Cu-Ag [15].

EXPERIMENTAL

Fe-Au alloys of stoichiometric Fe_xAu_{1-x} with nominal compositions $x = 0$, 0.03, 0.20, and 0.50 were prepared for INS measurements by arc-melting, as detailed in Ref. [13]. Because of the large neutron absorption cross section of Au, the ingots were cold-rolled to a thickness of 120 μm to ensure the transmission of neutrons through the sample. X-ray

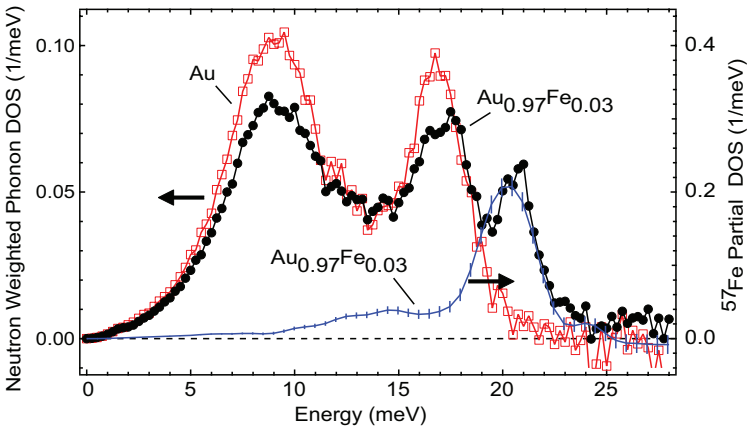

FIGURE 2. (color online) Experimental phonon DOS curves. Left axis is the neutron-weighted phonon DOS curves for pure Au and $Au_{0.97}Fe_{0.03}$ from INS measurements and the right axis is the ^{57}Fe partial phonon densities of states for $Au_{0.97}Fe_{0.03}$ from NRIXS measurements.

diffractometry confirmed all the samples to be in the fcc phase. Samples for NRIXS measurements were prepared in the same way for compositions $x = 0$, 0.03, 0.10, 0.20, 0.30, 0.40, 0.50, and 0.60, but they were 96.06% enriched with ^{57}Fe, a Mössbauer isotope. These ingots were cold-rolled to thicknesses between 10 and 50 μm.

INS measurements were performed with the wide Angular-Range Chopper Spectrometer [16] (ARCS) at the Spallation Neutron Source at Oak Ridge National Laboratory. The nominal incident neutron energy was 40 meV. The FWHM of the energy resolution was 1.6 meV at the elastic line, although the energy resolution of a direct energy spectrometer improves with increasing energy transfer. Details of the data collection [17] and reduction procedures using the DANSE software [18, 19] can be found elsewhere. NRIXS measurements were performed at beamline 16ID-D of the Advanced Photon Source at Argonne National Laboratory. The incident photon energy ranged from -80 to $+80$ meV in steps of 0.5 meV around the nuclear resonance energy of ^{57}Fe (14.413 keV). The monochromator resolution function was measured in situ and had a FWHM of 2.2 meV. The data was reduced using the PHOENIX code [20]. All neutron and x-ray measurements were performed at room temperature.

Different chemical elements have different neutron scattering efficiencies, so data obtained from INS are neutron-weighted. The neutron weights are the ratios of neutron cross section to molar mass, σ/M, which are 0.208 and 0.039 barns/amu for Fe and Au, respectively, so the motions of Fe atoms are overemphasized by a 5:1 ratio. A neutron-weight correction was made possible by combining the INS neutron-weighted phonon DOS spectra with the NRIXS Fe partial phonon DOS spectra, The curves in Fig. 1 show the neutron-weighted DOS curves along with the neutron-weight-corrected DOS curves and the Fe partial phonon DOS for the compositions $Fe_{0.20}Au_{0.80}$ and $Fe_{0.50}Au_{0.50}$. In Fig. 2, the neutron-weight correction is omitted for clarity and instead the Fe partial phonon DOS is plotted on the right axis to emphasize the similarities between the neutron and x-ray data.

RESULTS

The combination of INS and NRIXS measurements provides information of the individual motion of Au and Fe atoms. $S_{\rm vib}$ normalized by atom was obtained in the quasiharmonic formalism [21] from the normalized phonon DOS curves, $g(E)$, using

$$S_{\rm vib}(T)/\text{atom} = 3k_{\rm B}\int_0^\infty g(E)\left[(1+n_T(E))\ln(n_T(E)) - n_T(E)\ln(n_T(E))\right]dE\ , \tag{1}$$

where $n_T(E)$ is the Plank distribution at T, E is the phonon energy, $k_{\rm B}$ is Boltzmann's constant, and the integral effectively ends at the maximum phonon energy. The excess vibrational entropy of mixing as a function of Fe concentration x due to motions of atoms of type $h = \{\text{Au, Fe}\}$ in Fe_xAu_{1-x} is

$$\Delta S^h_{\rm vib}(x) = S^h_{\rm vib}(x) - \sigma^h_{\rm vib}\ , \tag{2}$$

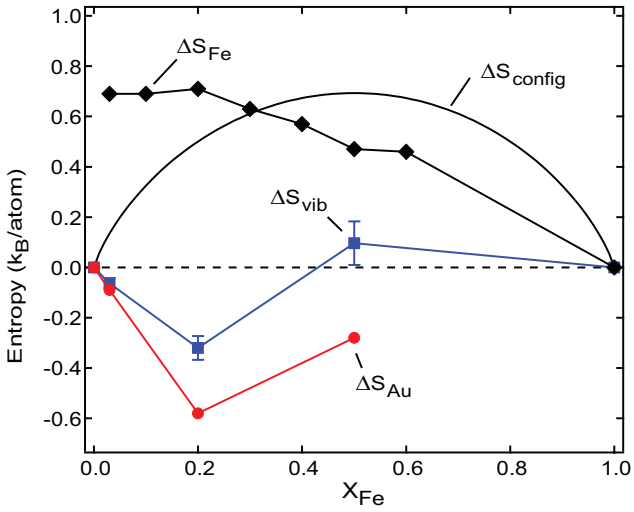

FIGURE 3. (color online) Configurational entropy of mixing ($\Delta S_{\rm config}$) and excess vibrational entropy of mixing ($\Delta S_{\rm vib}$) for Fe_xAu_{1-x} alloys with respect to ideal mixing of fcc Au and fcc Fe. Excess vibrational entropy contributions from Au and Fe are $\Delta S_{\rm Au}$ and $\Delta S_{\rm Fe}$.

where $\sigma^h_{\rm vib}$ is the vibrational entropy of pure element h. From the neutron scattering measurements we obtained $\sigma^{\rm Au}_{\rm vib} = 5.6\,k_{\rm B}$ per atom. Fe is not stable in the fcc structure at standard temperature and pressure, so we used the estimate discussed in Ref. [13] of $\sigma^{\rm Fe}_{\rm vib} = 3.5\,k_{\rm B}$ per atom. The excess vibrational entropy of mixing for the alloy Fe_xAu_{1-x} is the concentration-weighted sum of the curves obtained from Eq. 2 for Au and Fe motions

$$\Delta S^{\rm mix}_{\rm vib}(x) = [x]\,\Delta S^{\rm Fe}_{\rm vib}(x) + [1-x]\,\Delta S^{\rm Au}_{\rm vib}(x)\,. \tag{3}$$

The results are shown in Fig. 3. The magnitude of the excess phonon entropy of mixing is more than half the configurational entropy of mixing and opposite in sign. Although chemical mixing is favored in the fcc phase by the configurational entropy, the phonon entropy favors chemical unmixing, and contributes to the miscibility gap in the Fe-Au system.

WILLS-HARRISON MODEL

As shown in Fig. 3, $\Delta S^{\rm mix}_{\rm vib}(x)$ is negative in the Au-rich area, mostly because of the large stiffening of the Au partial phonon DOS. A simple way to study this phenomenon is by looking at the bulk modulus B, the resistance of a system to uniform compression, which is a measure of the stiffness of longitudinal long wavelength motions. It is given by

$$B = -V\frac{d^2U}{dV^2}\Big|_T\,, \tag{4}$$

where V is the volume. There are several contributions to the total energy U, and a textbook treatment of Au as a free-electron gas yields a bulk modulus of 35 GPa [22], but its experimental value is 171 GPa [23]. Hybridization between the s- and d-electrons accounts for the large difference. The Wills-Harrison model [14] provides an approximation of U for metals and includes contributions from the nearly-free-electron gas ($E_{\rm f}$), hybridization between the s-electrons and the d-band ($E_{\rm b}$), and nonorthogonality of hybridized d-states ($E_{\rm c}$). There are three model parameters: r_0, is the radius of a sphere equal to the atomic volume, r_d is an element-specific constant that describes the coupling of s- and d-electrons in the pseudopotential perturbation formalism [24], and r_c is the radius of the Ashcroft empty-core pseudopotential [25] which is a free parameter but related to the atom core radius. The nearly-free-electron gas contribution to the total energy is given by

$$E_{\rm f} = \frac{3}{5}Z_s\frac{\hbar^2}{2m}k_F^2 - \frac{3Z_se^2k_F}{4\pi} - \frac{Z_s^2e^2\alpha k_F}{(18\pi Z_s)^{1/3}} + \frac{2Z_s}{3\pi}e^2r_c^2k_F^3\,, \tag{5}$$

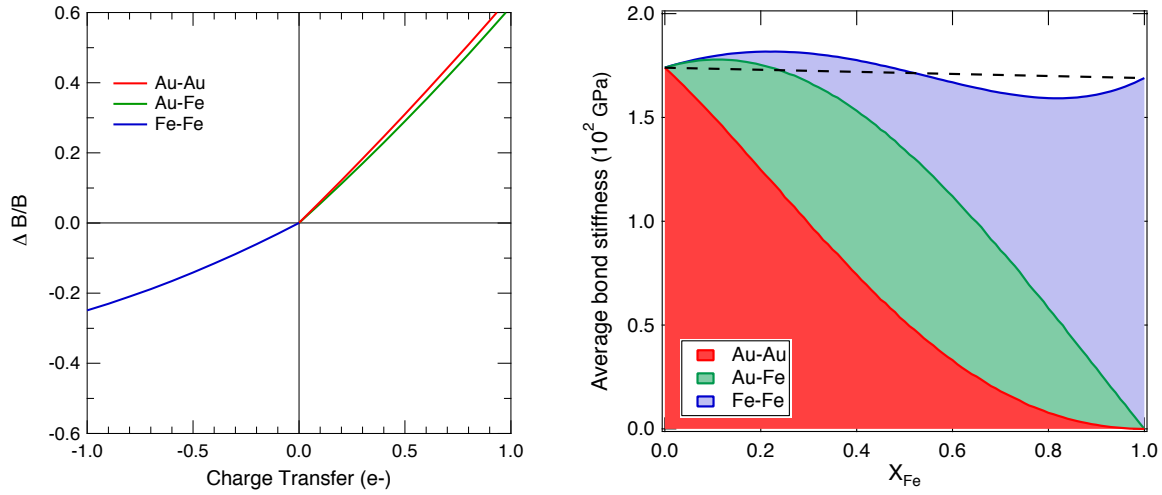

FIGURE 4. (color online) Left: Percent change of the bond stiffness when charge is increased or decreased in the atomic spheres of each pair of atoms in the Fe-Au system. Right: average bond stiffness predicted by the Wills-Harrison model as a function of Fe concentration and relative contribution from each kind of bond. The dashed line is the concentration-weighted average of the Au–Au and Au–Fe bonds.

where Z_s is the charge in the outermost s-electron shell, e and m are the electron charge and mass, α is the Madelung constant, and the Fermi wavevector k_F is

$$k_F = \frac{1}{r_0}\left(\frac{9\pi Z_s}{4}\right)^{1/3} . \tag{6}$$

On the right side of Eq. 5, the first term is the kinetic energy, the second term is the exchange energy, the third term is the Madelung energy, and the last term is a correction to the Madelung energy when used with the Ashcroft empty-core pseudopotential. The contributions from sd-hybridization and from the nonorthogonality of the hybridized d-states are

$$E_b = -\frac{1}{2}Z_d\left[1-\frac{Z_d}{10}\right](30.9)c^{1/2}\frac{\hbar^2 r_d^3}{m_e d^5} = -\frac{1}{2}Z_d\left[1-\frac{Z_d}{10}\right]W_d \tag{7}$$

and

$$E_c = Z_d c(11.4)\frac{\hbar^2 r_d^6}{m_e d^8} , \tag{8}$$

respectively. The numerical values arise from the d-state coupling, c is the number of first-nearest-neighbors for the crystal structure of the system, d is separation between first-neighbors, and $Z_d = Z - Z_s$ is the charge in the outermost d-electron shell, coupled to the total valence Z. Finally, $W_d = 10/N(\varepsilon)$ is a shape parameter that describes width of a rectangular d-band density of states in which the height is the number of electrons at the Fermi level $N(\varepsilon)$. W_d comes from the Friedel model and every element has a characteristic value [26].

We constructed a 'Wills-Harrison periodic table' [27] using values for r_0 and r_d originally tabulated by Wills and Harrison [14] and fitting r_c to obtain accurate bulk moduli for several elemental metals, which themselves were obtained by taking the appropriate derivates from the components of U. We used these values to calculate the bulk moduli of inter-element bonds using the geometric mean of r_0, r_d, and r_c for each pair. Several results are shown in Table 1. The Wills-Harrison model predicts that the Co–Fe and V–Fe bonds are softer than the average of Co–Co and Fe–Fe, and V–V and Fe–Fe bonds, respectively, which is accurate [28, 29] and typically results in an ordering tendency [30]. The model predicts that the Au–Fe bond in the fcc structure is softer than the average of Au–Au and Fe–Fe bonds, but Fe-Au is evidently a system with unmixing tendencies. The expected relationship between the stiffness of the bonds is recovered when charge transfer, which is negligible in the Fe-V and Fe-Co systems but significant in the Fe-Au system, is implemented in the model. This was done by varying Z_s and Z_d in essentially a rigid-band fashion. As shown in the plot on the left in Fig. 4, the Wills-Harrison model predicts an increase in the stiffness of the Au–Au and Fe–Au bonds when the charge is increased that is not completely offset by the softening of Fe–Fe bonds when the

TABLE 1. Total stiffness of the bond between several pairs of elements predicted by the Wills-Harrison model, and contributions from B_f, B_b, and B_c (see text for details). The values have units of GPa.

	Au–Au	**Au–Fe**	**Co–Co**	**Co–Fe**	**V–V**	**V–Fe**	**Fe–Fe**
B_f	58	158	272	291	352	330	309
B_b	-81	-179	-211	-227	-296	-303	-250
B_c	197	164	131	110	109	118	110
B	174	143	192	174	165	145	169

charge is reduced by the same amount. Based on the proportion of bonds and their stiffness, and using a value for the charge transfer of 0.04 e^- per Au–Fe bond, as estimated in Ref. [13], the average bond stiffness for the system was calculated as a function of Fe concentration and is shown on the right side of Fig. 4. The proportion coming from each kind of bond is also shown, with the contribution from the Au–Au bonds at the bottom, Au–Fe bonds in the middle, and Fe–Fe bonds at the top.

DISCUSSION

The vibrational entropies of pure Au and pure Fe can be used to obtain an ideal vibrational entropy of mixing of $-2.14\,k_B$/atom/(at. fraction Fe). However, a fit to the data in Fig. 3 up to 20 at. % Fe gives a slope of $-3.75\,k_B$/atom/(at. fraction Fe), 75% larger than the value from a simple substitution. A way to assess the thermodynamic effects of the vibrational entropy is by comparing the observed miscibility gap temperatures as a function of Fe content x, $T^{\text{mix}}_{\text{config + vib}}(x)$, which includes vibrational and configurational contributions, to those expected from configurational entropy alone, $T^{\text{mix}}_{\text{config}}(x)$,

$$T^{\text{mix}}_{\text{config + vib}}(x) = T^{\text{mix}}_{\text{config}}(x) \cdot \left(1 + \frac{\Delta S^{\text{mix}}_{\text{vib}}(x)}{\Delta S^{\text{mix}}_{\text{config}}(x)}\right)^{-1} , \tag{9}$$

where $\Delta S^{\text{mix}}_{\text{vib}}(x)$ is the excess vibrational entropy of mixing and $\Delta S^{\text{mix}}_{\text{config}}(x)$ is the configurational entropy of mixing, given in the point approximation by

$$\Delta S_{\text{config}}(x) = -k_B[(1-x)\ln(1-x) + x\ln(x)] . \tag{10}$$

Both of these quantities are plotted in Fig. 3. The plot on the left in Fig. 5 is a polynomial fit to the measured excess vibrational entropy of mixing and the expected configurational entropy (Eq. 10). It shows that S_{vib} is a main contributor to the observed miscibility gap temperature, especially at low Fe concentrations. It increases rapidly and peaks at about 10 at. % Fe, with a predicted 4.6-fold increase of about 550 K. After the peak, the magnitude of the effect decreases with increasing Fe concentration, and it is close zero at the equiatomic composition. The fit predicts a reversal of the effect of S_{vib} on the miscibility gap temperature in the Fe-rich region, but there are no data available and it is more difficult to satisfy the assumption that the underlying lattice is fcc. There are sources of uncertainty in the values such as short-range order which may decrease the configurational entropy and the the estimation of $\sigma^{\text{Fe}}_{\text{vib}}$ in the fcc structure, but this are expected to be small. The temperature dependence of the vibrational entropy is anharmonic in other systems with segregation tendencies like Cu-Ag [15], but high temperature data were not available to perform this analysis for Fe-Au.

The plot on the right in Fig. 5 shows that S_{vib} increases the miscibility gap temperature to the observed phase boundaries of the system [31] from the lower temperatures expected if only S_{config} were considered. The same analysis was performed for several alloys using the values calculated by Ozoliņš, Wolverton, and Zunger [32] and the results are presented in Table 2. The ratios between critical temperatures with and without vibrational entropy contributions is of the same order of magnitude as those observed in the Fe-Au system. The effect of the excess vibrational entropy of mixing is to decrease the miscibility gap temperature in $Cu_{0.859}Ag_{0.141}$ and NiAu. It increases the order-disorder transition temperature in AgAu and reduces it in CuAu.

The Wills-Harrison model predicts a value of 143 GPa for the bulk modulus of the Fe–Au bond, compared to 174 and 169 GPa for Au–Au and Fe–Fe bonds, respectively. This is in agreement with the ab initio calculations which predict that the Fe–Au bond is softer than the Au–Au bond [13]. For Au–Fe bonds, the relative weight of each contribution, B_f,

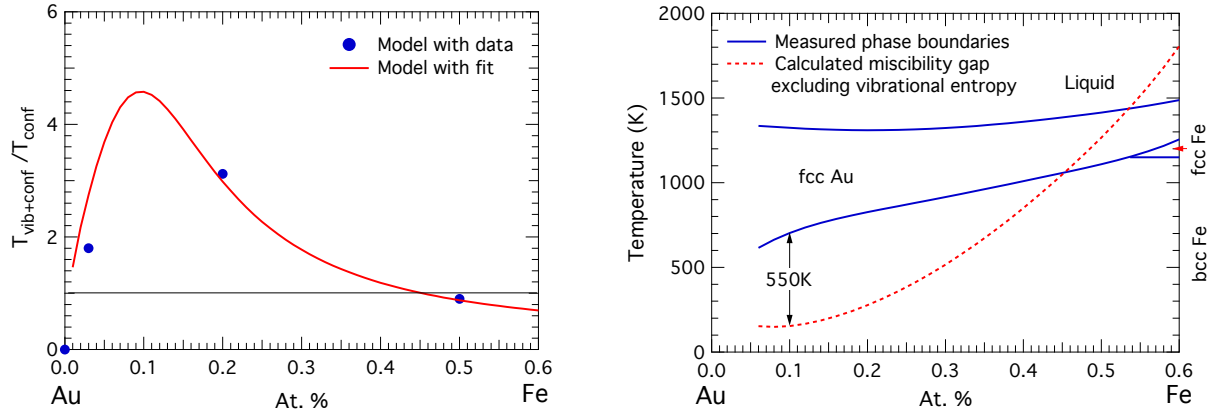

FIGURE 5. (color online) Left: Percent increase of the miscibility gap temperature as a function of Fe content in the Fe-Au system when considering vibrational and configurational entropies versus the configurational contribution alone. Right: Comparison of the observed phase boundaries with the calculated phase boundaries when only configurational entropy is considered.

B_b, and B_c, is intermediate between that of noble metal and transition metal bonds, and B_b and B_c almost cancel each other out. The Au partial phonon DOS stiffens with increasing Fe concentration (Fig. 3), so a stiffening of the Au–Au bonds is expected. Stiffening of both the Au–Au and Au–Fe bonds is predicted by the Wills-Harrison model when charge increases (Fig. 4) and it is due to an increase in the number of electronic *s*-states near the Fermi level and due to *sd*-hybridization. The former is more important for the Au–Fe bonds and the latter for the Au-Au bonds, so overall they are comparable in magnitude. Without any fits to the experimental data, the Wills-Harrison model with a constant charge transfer per Au–Fe bond successfully reproduces the Fe concentration dependence expected from an average bond in the Fe-Au system based on the measured excess vibrational entropy of mixing, and this is shown on the right in Fig. 4. This supports ideas developed here and elsewhere [13] that charge transfer is highly local, affects different bonds differently and independently, and the measured quantities depend mostly on the number and type of bonds in the system. The model predicts a reversal of the trend when Fe becomes the solvent, when the average of the bonds in the system is lower than that of pure Fe and the excess vibrational entropy of mixing should *decrease* the miscibility gap temperature. Perhaps it does to an extent, but there is no experimental data available and other obstacles to mixing gain prominence, such as the large size and mass mismatch between Fe and Au atoms. Additionally, as mentioned above, the stability of the underlying fcc lattice is questionable in this region. In Ni-Cu, it was predicted that the Cu partial phonon DOS stiffens monotonically with increasing Ni concentration whereas the Ni partial phonon DOS softens monotonically with increasing Cu content [9], so instead of a reversal, the excess vibrational entropy of mixing has a minimum around the equiatomic composition. This difference is likely to originate with the larger number of *d*-electrons of Ni compared to Fe.

CONCLUSION

The changes in the phonons of Fe and Au with increasing Fe composition in the Au-rich section of the Fe-Au binary system where investigated using INS and NRIXS. The phonon partial DOS of Au atoms depends strongly on the Fe concentration, with an increase in the average energy (stiffening) of the Au vibrations with increasing Fe content. The excess vibrational entropy of mixing of the system was estimated from these measurements. It is negative, thus increasing the miscibility gap temperature of the system, and has a minimum at a concentration of about 20 at.% Fe. The stiffening of the phonons is correlated to the stiffening of the bonds predicted by the Wills-Harrison model when accounting for a charge transfer from the Fe to the Au atoms. The Au–Fe bond is inherently soft but becomes stiffer than the average of the Fe–Fe and Au–Au bonds at Fe concentrations below 50 at.%, predicting chemical un-mixing in the system. The average bond stiffness, which depends on the concentration, has a maximum that corresponds to the minimum of the excess vibrational entropy of mixing. The bond stiffening occurs due to the donation of charge from Fe atoms to a nearly-free-electronic band and the increase in the number of available *d*-electrons from the Fe that

TABLE 2. Measured disordering temperature $T^{\mathrm{mix}}_{\mathrm{config+vib}}$ and disordering temperature accounting only for configurational entropy $T^{\mathrm{mix}}_{\mathrm{config}}$. Change in configurational entropy $\Delta S^{\mathrm{mix}}_{\mathrm{config}}$ and excess vibrational entropy of mixing $\Delta S^{\mathrm{mix}}_{\mathrm{vib}}$ upon disordering for the ordering systems CuAu and AgAu and the segregating systems $Cu_{0.859}Ag_{0.141}$ and NiAu. Shift in the disordering temperature due to vibrational entropy alone $T^{\mathrm{mix}}_{\mathrm{vib}}$. Temperatures are in K and entropies in k_B/atom.

	$T^{\mathrm{mix}}_{\mathrm{config+vib}}$	$\Delta S^{\mathrm{mix}}_{\mathrm{config}}$	$\Delta S^{\mathrm{mix}}_{\mathrm{vib}}$	$T^{\mathrm{mix}}_{\mathrm{config+vib}}/T^{\mathrm{mix}}_{\mathrm{config}}$	$T^{\mathrm{mix}}_{\mathrm{vib}}$
CuAu	800	0.57	0.16	0.78	-225
AgAu	800	0.62	-0.10	1.19	129
$Cu_{0.859}Ag_{0.141}$	1052	0.40	0.37	0.52	-973
NiAu	1100	0.56	0.48	0.54	-943

affects the *sd*-hybridization.

ACKNOWLEDGMENTS

We thank M. S. Lucas and L. Mauger for stimulating discussion, preparation and characterization of the samples, and help collecting the experimental data. We thank D. L. Abernathy, M. B. Stone and Y. Xiao for help collecting the experimental data. This work was supported by DOE BES under contract DE-FG02-03ER46055.

REFERENCES

1. F. Körmann, A. Breidi, S. Dudarev, N. Dupin, G. Ghosh, T. Hickel, P. Korzhavyi, J. A. Muñoz, and I. Ohnuma, *Phys. Stat. Sol. (b)* **251**, 53 (2014).
2. M. Bienzle, T. Oishi, and F. Sommer, *J. Alloys Compd.* **220**, 182 (1995).
3. C. Wolverton, and A. Zunger, *Comput. Mater. Sci.* **8**, 107 (1997).
4. C. Colinet, J. Eymery, A. Pasturel, A. T. Paxton, and M. van Schilfgaarde, *J. Phys.: Condens. Matter.* **6**, L47 (1994).
5. R. Tetot, and A. Finel, "The Gaussian Cluster Variation Method and Its Application to The Thermodynamics of Transition Metals," in *Stability of Materials*, edited by A. Gonis, P. Turchi, and J. Kudrnovsky, Springer, 1996, vol. 355 of *NATO ASI Series*, p. 197.
6. M. Asta, and S. M. Foiles, *Phys. Rev. B* **53**, 2389 (1996).
7. J. R. Clinton, E. H. Tyler, and H. L. Luo, *J. Phys. F: Met. Phys.* **4**, 1162 (1974).
8. R. A. Oriani, *Acta Metall.* **3**, 232 (1955).
9. B. Onat, and S. Durukanoğlu, *Eur. Phys. J. B* **87**, 264 (2014).
10. T. L. Swan-Wood, O. Delaire, and B. Fultz, *Phys. Rev. B* **72**, 024305 (2005).
11. O. Delaire, T. L. Swan-Wood, and B. Fultz, *Phys. Rev. Lett.* **93**, 185704 (2004).
12. B. H. de Mayo, *J. Phys. Chem. Solids* **35**, 1525 (1974).
13. J. A. Muñoz, M. S. Lucas, L. Mauger, I. Halevy, J. Horwath, S. L. Semiatin, Y. Xiao, P. Chow, M. B. Stone, D. L. Abernathy, and B. Fultz, *Phys. Rev. B* **87**, 014301 (2013).
14. J. M. Wills, and W. A. Harrison, *Phys. Rev. B* **28**, 4363 (1983).
15. J. Creuze, F. Berthier, R. Tétot, B. Legrand, and G. Tréglia, *Phys. Rev. B* **61**, 14470 (2000).
16. D. L. Abernathy, M. B. Stone, M. J. Loguillo, M. S. Lucas, O. Delaire, X. Tang, J. Y. Y. Lin, and B. Fultz, *Rev. Sci. Instr.* **83**, 015114 (2012).
17. M. S. Lucas, M. Kresch, R. Stevens, and B. Fultz, *Phys. Rev. B* **77**, 184303 (2008).
18. M. Kresch, O. Delaire, R. Stevens, J. Y. Y. Lin, and B. Fultz, *Phys. Rev. B* **75**, 104301 (2007).
19. B. Fultz, T. Kelley, J. Lin, J. Lee, O. Delaire, M. Kresch, M. McKerns, and M. Aivazis, Experimental inelastic neutron scattering: Introduction to DANSE, http://docs.danse.us/DrChops/ExperimentalInelasticNeutronScattering.pdf (2009).
20. W. Sturhahn, *Hyperfine Interact.* **125**, 149 (2000).
21. B. Fultz, *Prog. Mater. Sci.* **55**, 247 (2010).
22. N. W. Ashcroft, and N. D. Mermin, *Solid State Physics*, Holt, Rinehart and Winston, New York, 1976.
23. E. A. Brandes, and G. B. Brook, editors, *Smithells Metals Reference Book*, Butterworth-Heinemann Ltd., Oxford, 1992.
24. W. A. Harrison, and S. Froyen, *Phys. Rev. B* **21**, 3214 (1980).
25. N. W. Ashcroft, *Phys. Lett.* **23**, 48 (1966).
26. J. Friedel, "Transition metals: Electronic structure of the d-band," in *The Physics of Metals*, edited by J. M. Ziman, 1969.

27. J. A. Muñoz, *Electronic structure and phonon thermodynamics of iron alloys*, Ph.D. thesis, California Institute of Technology (2013).
28. M. S. Lucas, J. A. Muñoz, L. Mauger, C. W. Li, A. Sheets, Z. Turgut, J. Horwath, D. L. Abernathy, M. B. Stone, O. Delaire, Y. Xiao, and B. Fultz, *J. Appl. Phys.* **108**, 023519 (2010).
29. J. A. Muñoz, M. S. Lucas, O. Delaire, M. L. Winterrose, L. Mauger, C. W. Li, A. O. Sheets, M. B. Stone, D. L. Abernathy, Y. Xiao, P. Chow, and B. Fultz, *Phys. Rev. Lett.* **107**, 115501 (2011).
30. G. D. Garbulsky, and G. Ceder, *Phys. Rev. B* **53**, 8993 (1996).
31. H. Okamoto, T. B. Massalski, L. J. Swartzendruber, and P. A. Beck, Fe-Au, http://www1.asminternational.org/AsmEnterprise/ (1990).
32. V. Ozoliņš, C. Wolverton, and A. Zunger, *Phys. Rev. B* **57**, 6427 (1998).